

## Comparative morphology and molecular phylogeny of aplanochytrids (Labyrinthulomycota)

Celeste A. Leander<sup>a,\*</sup>, David Porter<sup>b</sup>, Brian S. Leander<sup>c</sup>

<sup>a</sup>Department of Botany, University of British Columbia, Vancouver, BC, Canada V6T 1Z4

<sup>b</sup>Department of Plant Sciences, University of Georgia, Athens, GA 30605, USA

<sup>c</sup>Program in Evolutionary Biology, Departments of Botany and Zoology, Canadian Institute for Advanced Research, University of British Columbia, Vancouver, BC, Canada V6T 1Z4

Received 19 April 2004; accepted 30 July 2004

### Abstract

Aplanochytrids comprise one of three major subgroups within the Labyrinthulomycota. We have surveyed the diversity of aplanochytrids and have discovered that most isolates are difficult to identify to species because of character plasticity and ambiguity. Ten isolates were studied using molecular phylogenies based on small subunit ribosomal gene sequences (SSU rDNA) and morphological characters derived from light microscopy, SEM and TEM (e.g., colony size, colony shape, colony pattern, agar penetration, cell shape, cell surface patterns, cell inclusion characteristics and ectoplasmic net morphology). Of these isolates, we could positively identify two of them to species, namely *Aplanochytrium yorkensis* (Perkins, 1973) Leander and Porter, 2000 and *A. minuta* (Watson and Raper, 1957) Leander and Porter, 2000. We used standardized conditions for growing aplanochytrid isolates in order to minimize environmentally induced phenotypic plasticity in our comparative studies of morphology. By mapping the morphological characters listed above onto a conservative phylogenetic topology derived from SSU rDNA sequences, we were able to identify several synapomorphies (e.g., gross colony characteristics and cell surface patterns) that serve as valuable taxonomic characters for the identification of species and specific clades of aplanochytrids.

© 2004 Elsevier GmbH. All rights reserved.

**Keywords:** *Aplanochytrium*; Character evolution; Labyrinthulomycota; Marine fungi; Stramenopiles; Molecular phylogeny

### Introduction

The Labyrinthulomycota is comprised of three distinct groups of marine heterotrophic stramenopiles that are readily distinguished on the basis of gross morphological characters and molecular phylogenetic data: labyrinthulids (slime nets), thraustochytrids and aplanochytrids (Honda et al. 1999; Leander and Porter 2000, 2001; Raghukumar 2002) (Fig. 1). Aplanochytrids

and thraustochytrids possess globose sporangia and multi-laminar scaly walls (Darley et al. 1973; Perkins 1973; Porter 1989). However, the vegetative cells of aplanochytrids are capable of crawling movement using ectoplasmic filaments that do not completely enrobe the cells, a characteristic that distinguishes aplanochytrids from labyrinthulids (which are enrobed by and glide through the ectoplasmic network) and thraustochytrids (which are immobile, except for the biflagellate spore stage) (Leander and Porter 2000, 2001).

Aplanochytrids are classified within a single genus, *Aplanochytrium*, which is defined by the crawling

\*Corresponding author. Fax: +1 604 822 6089.

E-mail address: [cleander@interchange.ubc.ca](mailto:cleander@interchange.ubc.ca) (C.A. Leander).

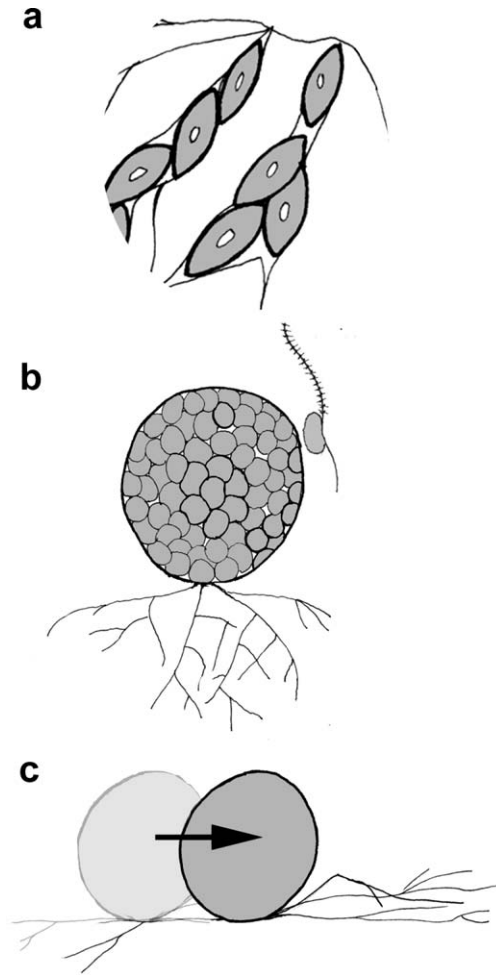


**Fig. 1.** Illustrations of the three major subgroups within the Labyrinthulomycota. (a) Labyrinthulids, as represented by *Labyrinthula* sp. with spindle-shaped vegetative cells enrobed by the ectoplasmic net. (b) Thraustochytrids, as represented by a non-proliferous *Thraustochytrium* sp. with unilateral non-motile ectoplasmic net. (c) Aplanochytrids, as represented by an *Aplanochytrium* sp. gliding via an ectoplasmic net.

movements and ectoplasmic net characteristics described above (Leander and Porter 2000). Aplanochytrids are most often associated with dead and decaying plant material, but some species are known to be pathogens of molluscs (Bower 1987). Although *Aplanochytrium* remained monotypic for 30 years (Bahnweg and Sparrow 1972), the transfer of five species from the genus *Labyrinthuloides* and one species from *Labyrinthula* to *Aplanochytrium* resulted in a total of seven species (Leander and Porter 2000). One new species, *A. stochinoi* Andreoli and Moro, 2003, has since been added (Moro et al. 2003), bringing the total number of recognized aplanochytrid species to eight. Nonetheless, identification of aplanochytrid species is difficult due to the plastic nature of fundamental morphological features. Important identification characters can change

depending on growth conditions, such as nutrients, temperature and salinity (Booth and Miller 1968; Wethered and Jennings 1985). Therefore, as an introduction to the overall diversity of the group, it is prudent to first summarize the diagnostic characteristics and culture conditions associated with the eight species described so far.

The type species of *Aplanochytrium*, *A. kerguelensis* Bahnweg and Sparrow, 1972 was originally isolated from sub-Antarctic waters and was grown in culture on pine pollen. The isolate was classified as a new genus because of the formation of spores that crawled along substrates, rather than highly motile biflagellated spores as seen in other members of the Labyrinthulomycota. Bahnweg and Sparrow (1972) used the term ‘aplanospores’ to describe the relative lack of motility present in *A. kerguelensis*, which formed the basis of the new genus name. However, the term ‘aplanospores’ generally refers to spores that are non-motile, so the term is perhaps inappropriate to describe the crawling spores of aplanochytrids. Accordingly, we have chosen to use the term ‘crawling spores’ from this point forward to refer to the defining property of aplanochytrids. Moreover, the definition of *Aplanochytrium* has since been modified to allow the inclusion of taxa that make biflagellate spores in addition to crawling spores (Leander and Porter 2000). The crawling spores of *A. kerguelensis* contain a large eccentric vacuole, which is a distinguishing character of the species, and a granular cytoplasm. The vacuole is also a conspicuous part of the developing sporangium. Ten to fifty crawling spores are released through rupture in the sporangial wall, or the spores germinate within the old sporangial wall to make clusters of sporangia. The ectoplasmic net is formed from several places on the spore body and extends in all directions.

*A. yorkensis* (Perkins, 1973) Leander and Porter, 2000 was isolated from oyster mantle, water samples, sediment and detritus and was maintained in axenic culture on a glucose/gelatin hydrolysate medium (Perkins 1973). Unlike *A. kerguelensis*, *A. yorkensis* makes biflagellate spores in addition to crawling spores. Perkins also described various membrane-bound inclusions within the cytoplasm, which might be the same structures as those causing the granular appearance in *A. kerguelensis*. *A. yorkensis* forms clumpy, cream-coloured colonies, and mature sporangia are rarely motile. The ectoplasmic net has two major radiating filaments that subsequently branch into finer threads.

*A. minuta* (Watson and Raper, 1957) Leander and Porter, 2000 was originally isolated from a green alga, *Ulva* sp. collected from the undersurface of a boat (Watson and Raper 1957). We have subsequently isolated *A. minuta* from many other substrates, including chlorophytes, rhodophytes, *Zostera marina* and sediments. The cells are more oblong than those of

*A. yorkensis* and *A. kerguelensis* and divide into tetrads. Biflagellate spores were not described in the original description, but have been reported since (Perkins 1974). *A. minuta* tends to spread in distinct rays as a monolayer over agar surfaces. Vegetative cells remain motile for the entire lifecycle, except during daughter cell formation, and have very fine ectoplasmic net elements (Watson and Raper 1957). Movement involves alternate reversal of direction.

*A. saliens* (Quick, 1974) Leander and Porter, 2000 was described from the marine grass *Halophila englemannii*; it was originally grown on a modified blood serum agar (Quick 1974a). *A. saliens* is relatively rare (found in two of 12 host plants), and has not been reported since the original description. The sporangia are spherical, but may be compartmentalized making the sporangium appear to have a rough texture. Four to twenty crawling spores are released via fissures in the wall of the sporangium and are characterized by the presence of an anterior pit. The shape of the cells is distinctive, with a pointed posterior and a rounded, inflated anterior. Colonies of *A. saliens* alternate between those rich in vegetative cells and those rich in sporangia. The colonies rich in vegetative cells embed in the agar and appear milky with concentric layers. Sporangia-rich colonies form white flecks (clusters of sporangia) that do not penetrate the agar surface. After about 5 days in culture, the sporangia-rich colonies become vegetative. The ectoplasmic net is described as being sub-dichotomously branched and entangled, but with a gently curved trunk that diverges into several thinner branches. Movement of vegetative cells is sporadic with intermittent rapid advances.

*A. schizochytrrops* (Quick, 1974) Leander and Porter, 2000 was isolated from the seagrass *Halodule wrightii* and grown on bovine serum agar (Quick 1974b). Although *A. schizochytrrops* is reported to be present on 50% of the sampled host plants, it has not been reported since its original description. Vegetative cells are spherical to ovoid and enlarge to produce sporangia that are spherical when single, but clump to form irregular masses. Vegetative cells have obvious large vacuoles. As an alternative to sporangium formation, vegetative cells can produce un-walled plasmodia, which fragment internally to produce sporangia or fragment completely into vegetative cells or new plasmodia. Like *A. saliens*, the sporangia consist of separate compartments, produce ectoplasmic networks that are straight and tapered. Also like *A. saliens*, *A. schizochytrrops* is characterized by vegetative cell-rich strains and sporangia-rich strains.

*A. haliotidis* (Bower, 1987) Leander and Porter, 2000 is a pathogen of abalone, but grows well in Eagle's minimal essential media (Bower 1987). Sporangia and vegetative cells are spherical and the cytoplasm contains few vesicles. Division is by binary fission; tetrads were not observed. Swellings along the ectoplasmic net are

typical. Unlike most aplanochytrids, crawling spores are not formed. Sporangia are readily made with the addition of seawater and three to ten biflagellate spores are released through a tear in the wall.

*A. thaisii* (Cox and Mackin, 1974; Leander and Porter, 2000) was described as a labyrinthulid. *A. thaisii* was isolated from the marine gastropod *Thais haemastoma floridana*, and was grown on beef serum agar (Cox and Mackin 1974). Like *A. saliens* and *A. schizochytrrops*, this species is characterized by sporangia-rich colonies alternating with vegetative cell-rich colonies. Both types of colonies occur in mono-layers. The vegetative colonies seem to be determinate, because they never return to a sporangial stage. Vegetative cells divide by binary or quaternary divisions, producing tetrads that are enveloped by a mucilaginous sheath. Sporangia are immobile with small reflective drops. Biflagellate spores are readily produced in the host tissue, but not on agar. Motile plasmodia are reported to pinch off new vegetative cells or fragment into many vegetative cells.

*A. stocchini* was collected in Antarctica on the thallus of the chlorophyte *Urospora* (Moro et al. 2003). Rhizoids are not visible with light microscopy, but SEM demonstrates that spherical vegetative cells attach to their substrate via an ectoplasmic net. Sporangia and vegetative cells are both surrounded by a multi-layered wall, and following complete cleavage, three to eight crawling spores are released via deliquescence of the sporangium wall. The spores crawl on moderately developed ectoplasmic net systems. Biflagellate spores have not been observed in this species.

During our survey of aplanochytrids, we have discovered several isolates with overlapping characters that fit more than one of the species descriptions above. Therefore, this study aims to clarify informative morphological characters and the phylogenetic relationships of aplanochytrids using ten aplanochytrid isolates collected from several different sites in the western Atlantic Ocean. We have developed standardized conditions for growing aplanochytrid isolates in order to generate a suite of morphological characters that can be used to identify newly encountered isolates to phylogenetic lineage based on morphology. Our approach combined electron microscopy, light microscopy, phylogenetic analyses of SSU rDNA sequences and phylogenetic mapping of morphological characters.

## Material and methods

### Collection of organisms and culture conditions

Most isolates used in this study were collected during 1998–99 from southern Florida, Puerto Rico and the

**Table 1.** Sequence accession numbers and collection information for members of the genus *Aplanochytrium* examined in this study

Taxon	Seq. length (bp)	Accession no. <sup>c</sup>	Substrate	Location
<i>A. kerguelensis</i> <sup>a</sup>	1787	AB022103	Unrecorded	Kerguelen Islands, South Indian Ocean
<i>A. stocchinoi</i> <sup>b</sup>	1762	AJ519935	<i>Urospora</i> sp.	Ross Sea, Antarctica
<i>A. minuta</i>	1802	L27634	<i>Zostera marina</i>	Middle Marsh, North Carolina
<i>Aplanochytrium</i> sp. SC1-1	1756	AF348520	<i>Rhizophora mangle</i>	Sweetings Cay, Bahamas
<i>A. yorkensis</i>	1225	AF265333	<i>Zostera marina</i>	Adams Point, New Hampshire
<i>Aplanochytrium</i> sp. M4-2	819	AY684799	<i>Syringodium filiforme</i>	Miami Harbor, Florida
<i>Aplanochytrium</i> sp. M8-6	868	AY684800	<i>Cladophora</i> sp.	Miami Harbor, Florida
<i>Aplanochytrium</i> sp. PR1-1	1700	AF348516	<i>Dictyota cervicornis</i>	San Juan, Puerto Rico
<i>Aplanochytrium</i> sp. PR12-3	1737	AF348517	<i>Chaetomorpha</i> sp.	San Juan, Puerto Rico
<i>Aplanochytrium</i> sp. PR15-1	1733	AF348518	<i>Thalassia testudinum</i>	San Juan, Puerto Rico
<i>Aplanochytrium</i> sp. PR24-1	1720	AF348519	<i>Syringodium filiforme</i>	San Juan, Puerto Rico
<i>Aplanochytrium</i> sp. SC24-1	1739	AF348521	<i>Thalassia testudinum</i>	Sweetings Cay, Bahamas

<sup>a</sup>Reference Bahnweg and Sparrow (1972) and Honda et al. (1999).

<sup>b</sup>Reference Moro et al. (2003).

<sup>c</sup>All GenBank accession numbers, except EMBL AJ519935 (*A. stocchinoi*).

Bahamas (Table 1). The *A. yorkensis* isolate was collected from New Hampshire in 1991. Different substrates were collected between the inter-tidal zone and a depth of 40 m and sealed in sterile bags. Substrates were then divided into small segments and placed on serum/seawater agar (SSA, 1% agar in sterile seawater and 0.01% horse serum). Growth was monitored over several days, and morphological characteristics of colonies and individual cells were measured on the eighth day. When colonies of aplanochytrids appeared, they were excised to new media and cryopreserved in liquid nitrogen. Thawed cultures were maintained on SSA for the duration of this study. When we could not positively identify an isolate to species due to overlapping or ambiguous character states, we used the isolate identification number in our records (Table 1). Cultures of each isolate have been cryopreserved and are maintained at the University of Georgia, Department of Botany Culture Collection of Fungi and Algae.

### Light and electron microscopy

Colony measurements and light microscopy of vegetative cells were performed on 8-day-old colonies. Low magnification images (10–60×) of aplanochytrid colonies were captured with the use of a reflective glass surface beneath the stereomicroscope stage that allowed for maximum light refraction. These image data were used to evaluate colony shape, pattern and agar penetration. Sections of colonies growing on 1% agar media were excised and placed directly on a standard glass slide with a small drop of seawater. Differential interference contrast (DIC) microscopy was used to evaluate characteristics including presence or absence of amoeboid cells, presence or absence of dense lipid drops

and refractive granules, and cell size and shape. Size measurements were taken from 10 separate transfers of each isolate.

In preparation for scanning electron microscopy (SEM), aplanochytrids were grown on Thermanox plastic cover slips (Nalge Nunc International, Rochester, NY) placed on the agar surface near the expanding edge of an established colony. The colonies on agar were fixed by saturating a piece of Whatman filter paper, mounted on the inside surface of a petri dish lid, with 4% OsO<sub>4</sub>. The colonies on agar were fixed by OsO<sub>4</sub> vapour for 30 min. Thermanox discs with fixed cells attached were removed from the agar, dehydrated through a standard ethanol series and critical point dried with CO<sub>2</sub>. The discs were then mounted on stubs and sputter coated with evaporated chromium. The cells were viewed under a LEO 982 scanning electron microscope.

In preparation for transmission electron microscopy (TEM), aplanochytrid cells were grown in liquid serum seawater broth (SSB, sterile seawater and 0.01% horse serum) for 1 week on a large cover glass sealed in a Gabridge chamber (Gabridge 1981). The medium was poured off and cells were pre-fixed for 30 min with 2% glutaraldehyde in a buffer consisting of 0.1 M sodium cacodylate and 1 M NaCl. Post-fixation was performed for 30 min with 1% OsO<sub>4</sub> in the same buffer. Both fixation steps were carried out at room temperature. Cells were dehydrated with a graded ethanol series, infiltrated with ethanol–resin mixtures and embedded in pure epoxy resin. The chamber was then placed in a 60 °C oven, where the resin was allowed to polymerize before being sectioned on a RMC MT-X ultramicrotome. Ultrathin sections were post-stained with uranyl acetate and lead citrate and viewed under a JEOL 100 CX II transmission electron microscope.



## DNA extraction, PCR amplification, alignment and phylogenetic analysis

Genomic DNA was isolated with a modified Chelex extraction protocol (Goff and Moon 1993). Cultures were grown for an average of 2 weeks on 1% SSA media. Small segments of the colony were excised from the agar, added to 200  $\mu$ l of chelex extraction buffer and incubated at 75 °C for 30 min. The extracts were then boiled for 10 min in a water bath before being cooled on ice for 5 min. After centrifugation, the top layer was removed and immediately used as a PCR template.

We used an overlapping combination of two primer sets, NS1–NS4 and NS3–NS8 (White et al. 1990) for PCR amplification on a Perkin-Elmer PCR System 2400. With both primer sets, an annealing temperature of 54 °C preceded an extension time of 1 min at 72 °C for 25 cycles. PCR products were sequenced directly in both directions using the above primer sets on a Perkin-Elmer ABI 377 following the manufacturer's protocols.

Alignment of new SSU rDNA sequences from the aplanochytrid isolates (Table 1) was performed using the ClustalW package available from the Genetics Computing Group, Madison, WI. Fine alignment was finished by eye. We focused on an alignment consisting of 10 aplanochytrid sequences and 2 outgroup taxa (representative thraustochytrids) producing a 12-taxon alignment containing 1615 sites in order to minimize artifacts of long-branch attraction (LBA) and to perform a more comprehensive analysis of aplanochytrid relationships. Sequences from two isolates were incomplete, namely *Aplanochytrium* sp. M8-6 and the isolate identified as *A. yorkensis* (Table 1). Accordingly, we also analyzed a 14-taxon alignment containing 12 aplanochytrid sequences, 2 outgroup taxa and 824 sites.

Maximum likelihood (ML) and distance methods under different DNA substitution models were performed on the alignments. The alpha shape parameters were estimated from the data using HKY and a gamma distribution with invariable sites and eight rate categories (alpha = 0.47 and Ti/Tv = 1.15 for the 12-taxon alignment and alpha = 0.54 and Ti/Tv = 1.17 for the 14-taxon alignment; fraction of invariable sites was zero for both alignments). Gamma-corrected ML trees (analyzed using the parameters listed above) were constructed with PAUP\* 4.0 using the general time reversible (GTR) model for base (Posada and Crandall 1998; Swofford 1999). Gamma corrected ML trees found with HKY and GTR were identical. ML bootstrap analyses were performed in PAUP\* 4.0 (Swofford 1999) on one hundred re-sampled data sets under an HKY model using the alpha shape parameter and transition/transversion ratio (Ti/Tv) estimated from the original data set.

Distances for both SSU rDNA data sets were calculated with TREE-PUZZLE 5.0 using the HKY

substitution matrix (Strimmer and Von Haeseler 1996) and with PAUP\* 4.0 using the GTR model. Distance trees were constructed with weighted neighbour joining (W NJ) using Weighbor (Bruno et al. 2000). Five hundred bootstrap data sets were generated with SEQBOOT (Felsenstein 1993). Respective distances were calculated with the shell script 'puzzleboot' (M. Holder and A. Roger, [www.tree-puzzle.de](http://www.tree-puzzle.de)) using the alpha shape parameter and transition/transversion ratios estimated from the original data sets and analyzed with Weighbor.

We also examined the 12-taxon and 14-taxon data sets with Bayesian analysis using the program MrBayes 3.0 (Huelsenbeck and Ronquist 2001). The program was set to operate with GTR, a gamma distribution and four MCMC chains (default temperature = 0.2). A total of 1,000,000 generations were calculated with trees sampled every 100 generations and with a prior burn-in of 20,000 generations, giving a total of 200 sampled trees. The approximate  $-\ln L$  values converged at a value of 5180 for the 12-taxon data set and 5775 for the 14-taxon data set. The 10,000 sampled trees were imported into PAUP\*, and a majority rule consensus tree was constructed from the 200 post-burn-in trees. Posterior probabilities were derived from the number of trees that displayed the most commonly encountered branching pattern for the particular nodes in question.

## Results and discussion

### General morphology of aplanochytrid isolates

Fig. 2 shows the morphological differences of colonies for the isolates examined in this study; these are also summarised in Table 2. The micrographs show two general patterns in colony growth: (1) colonies form distinct rays sprawling from the centre outward (Figs. 2a and b) or (2) colonies form clumps of cells on the agar without a radial pattern (Figs. 2c–e). Colonies from isolates PR24-1, *A. minuta*, PR15-1, M8-6 and SC24-1 had fine rays extending from the centre outwards (Fig. 2a). Colonies from isolates PR1-1 and PR12-3 were also organized rays, but they were thicker and meandering (Fig. 2b). Colonies of *A. yorkensis* had no rays, but instead were organized as large clumps of cells on the agar (Fig. 2d). Colonies of isolate SC1-1 were also arranged as clumps of cells on agar, but the clumps were significantly smaller than those of *A. yorkensis* (Fig. 2c). At the other morphological extreme were the colonies of isolate M4-2, which were organized as very dense layers of cells (Fig. 2e). Isolates SC1-1 and M4-2 readily penetrated the agar throughout the entire colony. This characteristic was not seen in any of the other isolates

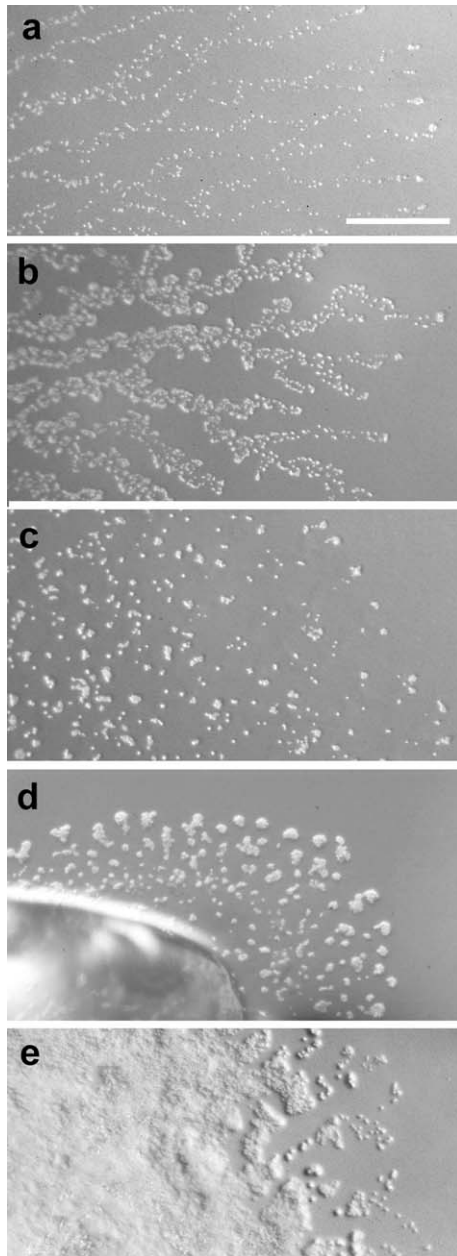


**Fig. 2.** Light micrographs showing colony morphology of aplanochytrids that were grown on a 1% standard serum seawater agar (i.e. not broth) medium for 8 days (all images at same scale, Bar=4 mm). (a) *A. minuta* showing straight narrow rays and an even margin. (b) Isolate PR1-1 showing meandering broad rays and an uneven margin. (c) Isolate SC1-1 showing small patches of cells and an even margin. (d) *A. yorkensis* showing large patches of cells and an even margin. (e) Isolate M4-2 showing a dense sheet of cells and an uneven margin.

we examined or in any previously described species (Table 2).

Selected light micrograph of vegetative cells of several aplanochytrid isolates are shown in Fig. 3. Cell shape varied from spherical (e.g., *A. yorkensis*, isolates PR1-1,

M4-2 (Fig. 3b) and SC24-1 (Fig. 3a)) to oblong (*A. minuta* (Fig. 3d), isolates PR12-3, PR24-1, M8-6 (Fig. 3c) and PR15-1) (Table 2); cells from isolate SC1-1 were sub-spherical in shape (Fig. 3e). Isolates M8-6, PR24-1 and PR12-3 had few cells that were weakly amoeboid. Some isolates (e.g., M8-6, PR24-1, PR15-1 and PR12-3) had occasional cells that were much larger than the more common vegetative cells. Many isolates, particularly isolate M4-2, had cells full of inclusions (e.g., Fig. 3b). Isolates PR15-1 and PR12-3 had inclusions that were obvious in the larger cells, but absent from smaller vegetative cells. Cell length ranged from an average of 2.4  $\mu\text{m}$  in isolate SC24-1 to 5.5  $\mu\text{m}$  in isolate PR24-1 (Table 2). Cells that were oblong in shape were larger than spherical cells, while the sub-spherical cells of isolate SC1-1 were intermediate in size.

The ectoplasmic network of the isolates was examined with SEM using chromium sputter coating. Isolates with spherical and sub-spherical cells (e.g., *A. yorkensis*, isolate M4-2 and isolate SC1-1) were covered with a very fine web-like ectoplasmic network (Figs. 4b, g–h). The ectoplasmic network of isolates SC24-1, PR1-1, PR24-1, PR12-3, PR15-1 and *A. minuta* consisted of broad, flattened filaments that were interrupted by nodular structures (Figs. 4d–f). SEM of aplanochytrids using chromium sputter coating also demonstrated a pattern of polygonal shapes that covered the entire surface of vegetative cells. The raised edges defining the polygons were continuous with the filaments of the ectoplasmic network (Figs. 4a–f). This pattern was not seen in SEM micrographs of either the thraustochytrid *Schizochytrium aggregatum* or the labyrinthulid *Labyrinthula* sp., and was essentially imperceptible when aplanochytrids were sputter coated with gold. TEM micrographs of the aplanochytrid cell surface confirmed that the polygonal patterns observed with SEM were not a manifestation of the overlapping organization of underlying scale layers (Fig. 4i).

### Molecular phylogeny of aplanochytrids based on small subunit rDNA

The inclusion of several isolates of *Aplanochytrium* species to a global alignment containing diverse eukaryotic representatives established aplanochytrids as a highly supported monophyletic group that is distinct from thraustochytrids (data not shown; Honda et al. 1999; Leander and Porter 2001, 2000). The 12-taxon alignment produced a well-resolved tree showing *A. kerguelensis* as the earliest diverging aplanochytrid that is followed by the divergence of clade A, which consists of isolates SC1-1 and M4-2 (Fig. 5a). *A. stocchinoi* diverged as the sister lineage to clade B, which consists of *A. minuta* and five related isolates collected and sequenced in this study (PR15-1, PR24-1,

**Table 2.** Morphological characters of species of *Aplanochytrium* examined in this study

Taxon	Average colony diameter (cm)	Colony margin shape	Colony pattern	1% Agar penetration	Cell shape	Average cell length (µm)	Inclusion	Ectoplasmic network
<i>A. minuta</i> (PR6-2)	4.1	Even, smooth	Straight, mid-sized rays	Superficial at centre of older colonies	Oblong	4.6	Small, few	Fine, with broad, flat areas
<i>Aplanochytrium</i> sp. PR15-1	3.6	Even, smooth	Straight, narrow rays	None	Oblong	5.3	In larger cells	Fine, with broad, flat areas
<i>Aplanochytrium</i> sp. SC24-1	2.8	Even, smooth	Straight, narrow rays	None	Spherical	2.4	Small, many	Flat, broad extension covering cells
<i>Aplanochytrium</i> sp. PR12-3	3.3	Slightly uneven	Curving, wide rays	Superficial at centre of older colonies	Oblong	5.0	In larger cells	Fine, with broad, flat areas
<i>Aplanochytrium</i> sp. PR1-1	3.2	Uneven, rough	Curving, wide rays	Superficial at centre of older colonies	Spherical	3.0	Some in all cells	Fine filaments, and web-like covering cells
<i>Aplanochytrium</i> sp. M8-6	2.6	Even, smooth	Slightly curving, narrow rays	Superficial at centre of older colonies	Oblong	4.1	Small, few	Fine, with beads
<i>Aplanochytrium</i> sp. PR24-1	2.8	Even, smooth	Curving, narrow rays	Superficial at centre of older colonies	Oblong	5.5	Small, few	Fine, with broad, flat areas
<i>Aplanochytrium</i> sp. SC1-1	1.7	Even, smooth	Small clumps	Profuse	Sub-spherical	4.4	Small, many	Fine filaments, and web-like covering cells
<i>Aplanochytrium</i> sp. M4-2	0.9	Uneven, rough	Dense sheet	Profuse	Spherical	2.7	Large, many	Fine with beads, and web-like covering cells
<i>A. yorkensis</i>	0.6	Even, less smooth	Large clumps	Limited to centre of older colonies	Spherical	4.3	Large, many	Fine filaments, and web-like covering cells

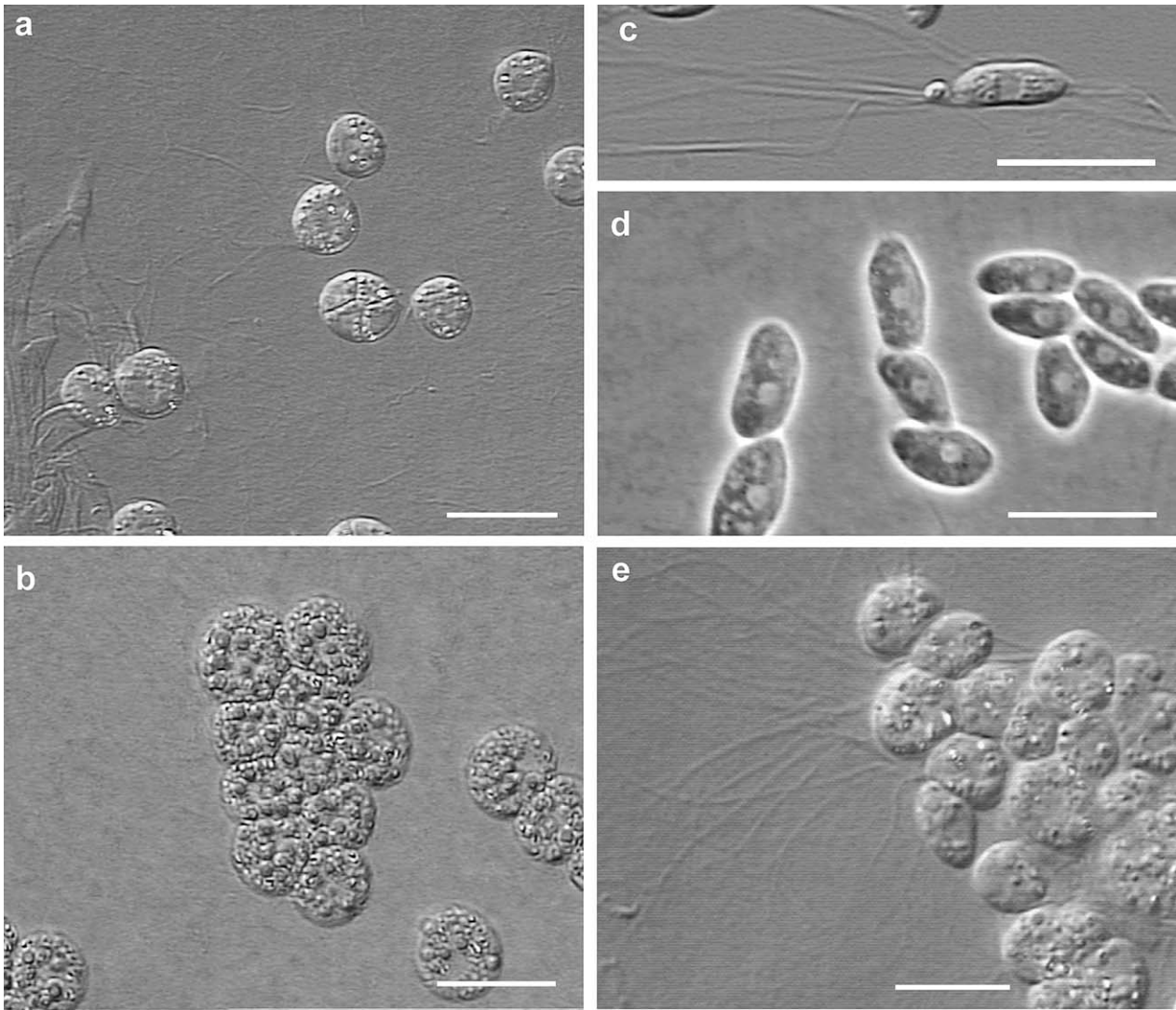


**Fig. 3.** Light micrographs showing variation in aplanochytrid cell shapes when grown on a standard serum seawater agar medium. (a) Differential interference contrast (DIC) image of isolate SC24-1 showing spherical cells (Bar = 3  $\mu$ m). (b) DIC image of isolate M4-2 showing spherical cells with many large refractive inclusions (Bar = 3  $\mu$ m). (c) DIC image of isolate M8-6 showing an oblong cell gliding on broad ectoplasmic filaments (Bar = 5  $\mu$ m). (d) Phase contrast image showing the oblong cells of *A. minuta* (Bar = 5  $\mu$ m). (e) DIC image showing the sub-spherical cells and ectoplasmic network (left side of image) of isolate SC1-1 (Bar = 5  $\mu$ m).

SC24-1, PR1-1 and PR12-3) (Fig. 5a; Moro et al. 2003). Clade **B** was bolstered by signature nucleotides at positions 336 and 344 and an signature indel at position 190 (relative to the SSU rDNA sequence from *A. minuta*). A shorter alignment (the 14-taxon alignment) enabled us to analyze the phylogenetic positions of two additional isolates: *A. yorkensis* and isolate M8-6 (Fig. 5b). Analyses of this data set consistently placed *A. yorkensis* and *A. kerquelenensis* together, forming clade **C**, which is consistent with morphological data (Bahnweg and Sparrow 1972; Perkins 1973; Ulken et al. 1985; Bahnweg and Jäckle 1986; Leander and Porter 2001). However, the bootstrap values supporting clade **C** were not strong. Moreover, ML and Bayesian analyses

favoured a sister relationship between clades **A** and **C**, the '*A. yorkensis* complex', albeit without statistical support (Fig. 5b). The relationship between clades **A** and **C**, however, was bolstered by signature nucleotides at positions 706 and 751 (relative to the SSU rDNA sequence from *A. minuta*). Isolate M8-6 consistently diverged with moderate to high statistical support as the sister group to clade **B**, forming the larger clade **D** – the '*A. minuta* complex' (Fig. 5b). Clade **D** was bolstered by a signature nucleotide at position 691 and signature indels at positions 185–186 and 191–196 (relative to the SSU rDNA sequence from *A. minuta*). In both the 12-taxon and 14-taxon data sets, isolates PR1-1 and PR12-3 formed a strongly supported clade **E** within clade **B**.



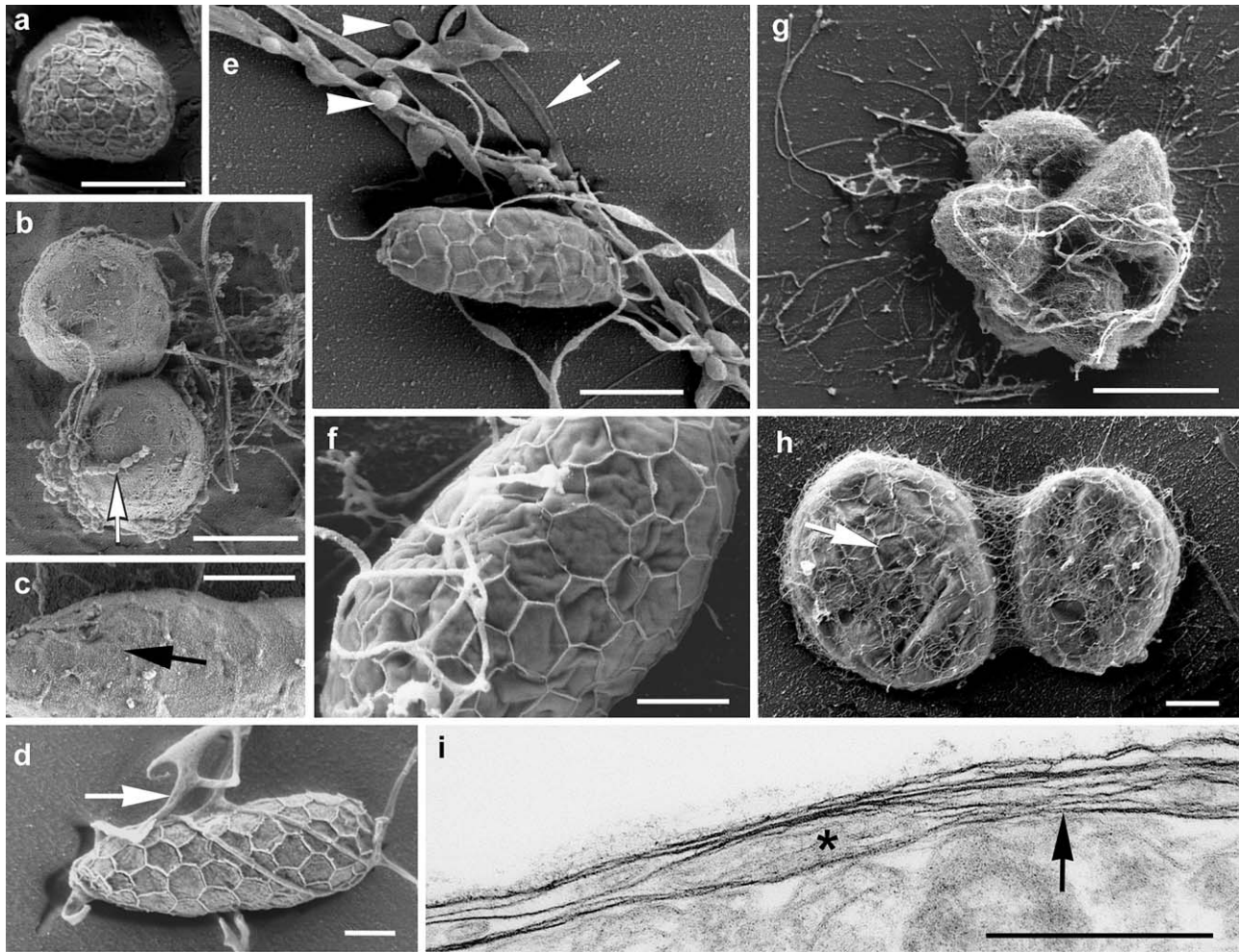


**Fig. 4.** Scanning electron micrographs of aplanochytrids showing surface patterns on vegetative cells and properties of the ectoplasmic network. (a) The cell surface of isolate SC24-1 showing a distinctive pattern of polygons visible with chromium-based sputter coating (Bar = 2  $\mu\text{m}$ ). (b, c) The cell surface of isolate M4-2 showing beaded ectoplasmic filaments (b, arrow) and distinctive polygons (c, arrow) that are barely visible using gold-based sputter coating (Bar = 2  $\mu\text{m}$  for both images). (d) The cell surface of isolate PR15-1 showing a distinctive pattern of polygons and broad ectoplasmic filaments (arrow) (Bar = 1  $\mu\text{m}$ ). (e) The cell surface of isolate *A. minuta* showing a distinctive pattern of polygons and broad ectoplasmic filaments (arrow) interrupted by nodular structures (arrowheads) (Bar = 2  $\mu\text{m}$ ). (f) The cell surface of isolate PR24-1 showing a distinctive pattern of polygons visible with chromium-based sputter coating (Bar = 1  $\mu\text{m}$ ). The raised edges of the polygons in (a)–(f) are continuous with the filaments of the ectoplasmic network. (g) Cell cluster of isolate SC1-1 showing sub-spherical cell shape and a covering of fine ectoplasmic net elements (Bar = 5  $\mu\text{m}$ ). (h) Two cells of isolate SC1-1 showing a polygonal surface pattern (arrow) under the fine web-like ectoplasmic covering (Bar = 1  $\mu\text{m}$ ). (i) Transmission electron micrograph of the cell wall of isolate SC1-1 showing an area of many overlapping scales (arrow) near an area of few overlapping scales (asterisk) (Bar = 0.5  $\mu\text{m}$ ).

### Character evolution in aplanochytrids

A synthesis of morphological data with the molecular phylogenetic relationships described above suggests that aplanochytrids form several clades that can be identified with synapomorphies associated with gross colony characteristics (Fig. 6). Aplanochytrid colonies tend to have either rays originating from the centre of the colony and extending outwards as in the *A. minuta* complex (clade D) or patches of cell clusters as found in the *A. yorkensis* complex (clades A and C). Moreover,

members of clade E, containing isolates PR1-1 and PR12-3, have rays that are broader than those seen in the other isolates of the *A. minuta* complex (clade D) (Fig. 6). Members of clade A share the ability to penetrate an agar substrate throughout the colony and possess several plesiomorphic features, including a spherical to sub-spherical cell-shape and relatively small cell size. Members of the *A. yorkensis* complex (clades A and C) possess a fine web-like ectoplasmic network over the cells, which is significantly different from the flattened ectoplasmic filaments found in members of

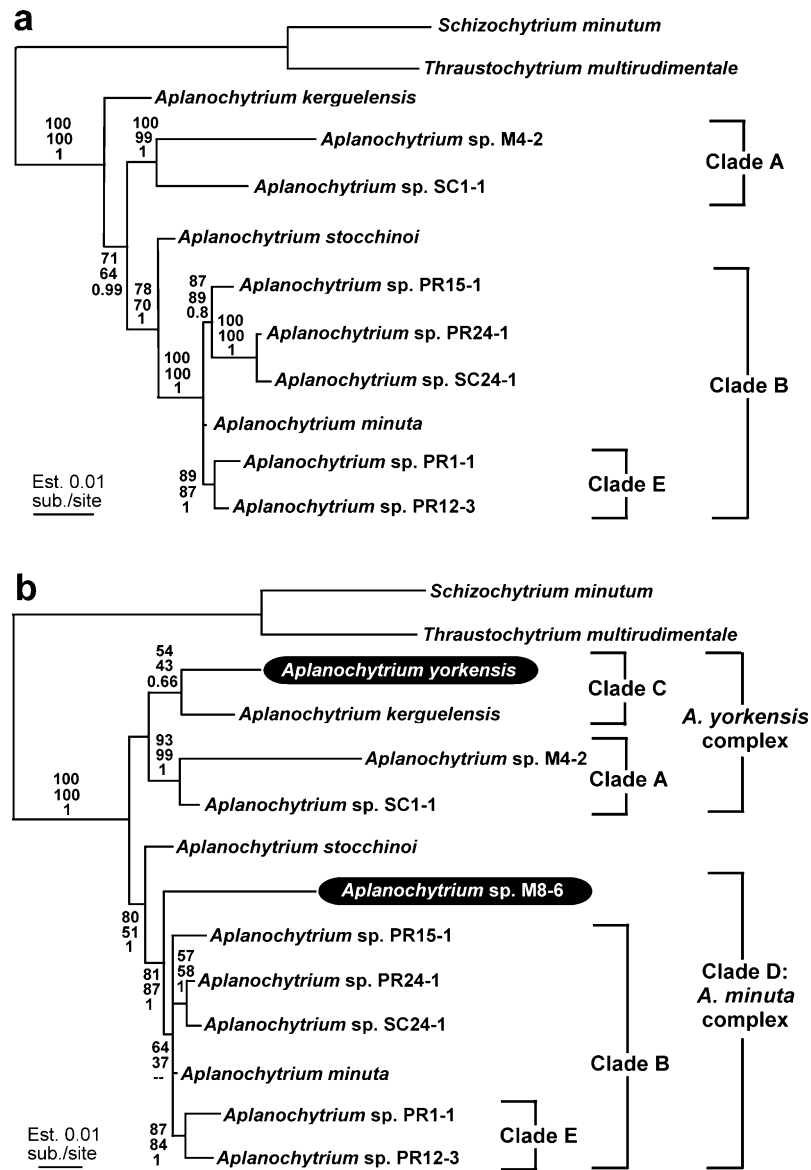


**Fig. 5.** Phylogenetic trees showing the relationships of aplanochytrids as inferred from small subunit (SSU) rDNA sequences. Numbers at the branches denote gamma-corrected bootstrap percentages using ML – HKY (upper) and weighted neighbor-joining (middle). The lower number refers to Bayesian posterior probabilities – GTR. (a) Gamma-corrected ML tree ( $-\ln L = 4057.5482$ ) inferred using the GTR model of substitution on an alignment of 12 SSU rDNA sequences and 1615 sites – the 12-taxon alignment. (b) Gamma-corrected ML tree ( $-\ln L = 2275.5777$ ) inferred using the GTR model of substitution on an alignment of 14 SSU rDNA sequences and 824 sites – the 14-taxon alignment.

the *A. minuta* complex (clade D). The two different structures of ectoplasmic nets correspond to different cell shapes: spherical cells are associated with fine web-like networks that cover the cells and naked oblong cells are associated with flattened ectoplasmic filaments. Because it is unclear whether the *A. yorkensis* complex (clades A and C) forms a monophyletic group or represents a paraphyletic grade, the colony and ectoplasmic net characteristics of the ancestral aplanochytrid are equivocal (step 1, Fig. 6). Nonetheless, putative synapomorphies for the aplanochytrids include an ectoplasmic network within or over which cells crawl

(Leander and Porter 2000), a cell wall comprised mainly of fucose (Honda et al. 1999) and a polygonal cell surface pattern (Figs. 4 and 6).

Understanding the phylogenetic distribution of the three characters listed above within the Labyrinthulomycota requires studies on more species. Nonetheless, the polygonal array of ectoplasmic filaments on the surface of aplanochytrids is curious. Like aplanochytrids, thraustochytrids also have a multi-layered cell wall made of overlapping polysaccharide scales. However, polygonal ectoplasmic filament patterns have not been observed in thraustochytrids (Harrison and Jones 1974),

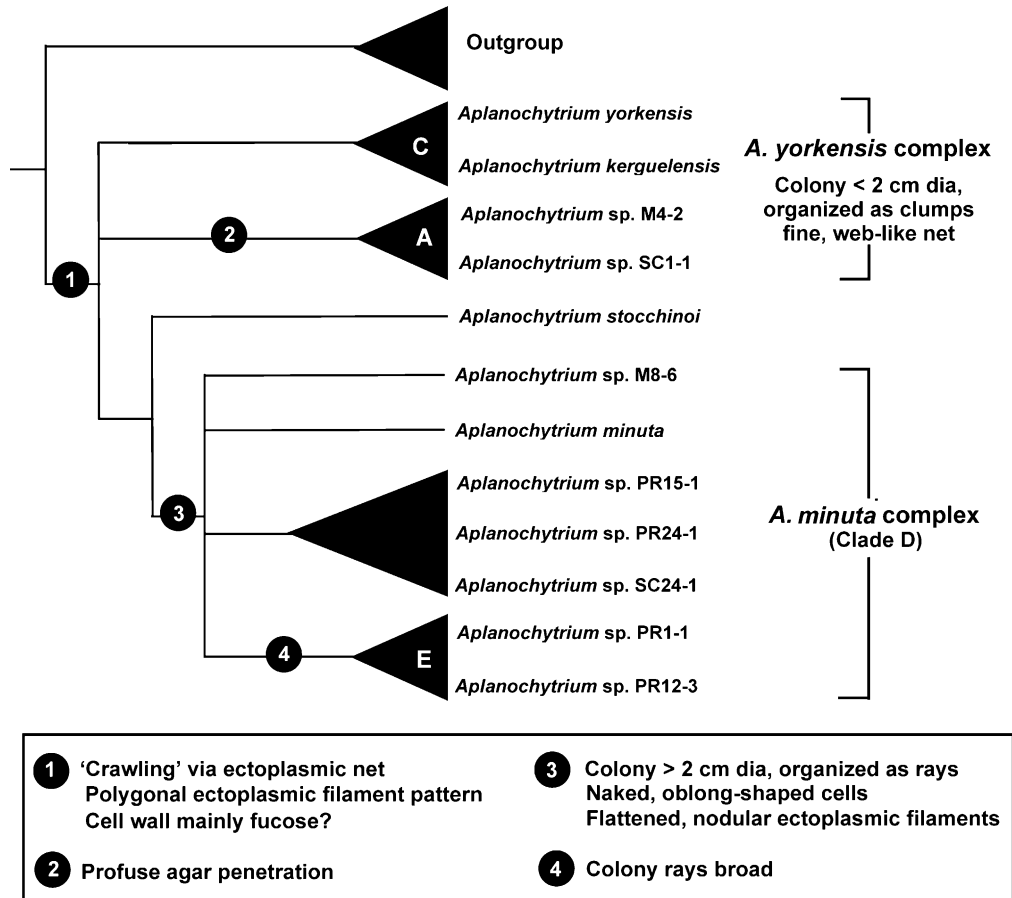


**Fig. 6.** Synthetic phylogenetic topology of aplanochytrids based on the molecular phylogenetic analyses presented in this study. Most of the morphological characters associated with colony formation, vegetative cells and the ectoplasmic network (Table 2) have been parsimoniously mapped onto the tree. Numbers refer to the specific characters listed in the box, and letters refer to the clades identified in Fig. 5.

which corresponds to their inability to move. It seems unlikely that labyrinthulids would possess the polygonal pattern, because their spindle-shaped cells are completely enrobed by the ectoplasmic net. It is interesting to note that scaly cell walls and polygonal cell surface patterns are frequently encountered in other stramenopiles and in haptophytes, cryptomonads and alveolates, particularly dinoflagellates (i.e., 'chromalveolates'). Although the ubiquity of these features are certainly the result of convergent evolution, much more structural and molecular phylogenetic evidence will be required before we are able to build the robust framework necessary for inferring the evolutionary histories of these cell surface characteristics.

## Acknowledgements

Collections in Bahamas were made possible by a grant from the NSF to Joseph Pawlik (OCE9711255), which provided UNOLS support of the R/V *Seward Johnson*.

We thank the government of the Bahamas for permission to perform research in their territorial waters. This work was supported in part by a Training Grant to C.A.L. in Molecular and Cellular Mycology (T32-AI-07373) from the National Institute of Health. B.S.L. was supported by the Natural Sciences and Engineering Research Council of Canada (283091-04) and the Canadian Institute for Advanced Research, Program in Evolutionary Biology.

## References

- Bahnweg, G., Sparrow, F.K., 1972. *Aplanochytrium kerguelensis* gen. nov. spec. nov., a new phycomyceete from subantarctic marine waters. Arch. Mikrobiol. 81, 45–49.
- Bahnweg, G., Jäckle, I., 1986. A new approach to the taxonomy of the Thraustochytriales and Labyrinthulales. In: Moss, S.T. (Ed.), The Biology of Marine Fungi. Cambridge University Press, Cambridge, pp. 131–140.

- Booth, T., Miller, C.E., 1968. Comparative morphologic and taxonomic studies in the genus *Thraustochytrium*. *Mycologia* 60, 480–495.
- Bower, S.M., 1987. *Labyrinthuloides haliotidis* n. sp. (Protozoa: Labyrinthomorpha), a pathogenic parasite of small, juvenile abalone in a British Columbia mariculture facility. *Can. J. Zool.* 65, 1996–2007.
- Bruno, W.J., Socci, N.D., Halpern, A.L., 2000. Weighted neighbor joining: a likelihood-based approach to distance-based phylogeny reconstruction. *Mol. Biol. Evol.* 17, 189–197.
- Cox, B., Mackin, J., 1974. Studies on a new species of *Labyrinthula* (Labyrinthulales) isolated from the marine gastropod *Thais haemastoma floridana*. *Trans. Am. Microsc. Soc.* 93, 62–70.
- Darley, W.M., Porter, D., Fuller, M.S., 1973. Cell wall composition and synthesis via Golgi-directed scale formation in the marine eukaryote, *Schizochytrium aggregatum*, with a note on *Thraustochytrium* sp. *Arch. Mikrobiol.* 90, 89–106.
- Felsenstein, J., 1993. PHYLIP (Phylogeny Inference Package). University of Washington, Seattle, Washington.
- Gabridge, M.G., 1981. The chamber/dish: an improved vessel for cell and explant tissue. *In Vitro* 17, 91–97.
- Goff, L.F., Moon, D.A., 1993. PCR amplification of nuclear and plastid genes from algal herbarium specimens and algal spores. *J. Phycol.* 29, 381–384.
- Harrison, J.L., Jones, E.B.G., 1974. Zoospore discharge in *Thraustochytrium striatum*. *Trans. Br. Mycol. Soc.* 62, 283–288.
- Honda, D., Yokochi, T., Nakahara, T., Raghukumar, S., Nakagiri, A., Schaumann, K., Higashihara, T., 1999. Molecular phylogeny of labyrinthulids and thraustochytrids based on the sequencing of 18S ribosomal RNA gene. *J. Eukaryot. Microbiol.* 46, 637–647.
- Huelsenbeck, J.P., Ronquist, F., 2001. MrBayes: Bayesian inference of phylogenetic trees. *Bioinformatics* 17, 754–755.
- Leander, C., Porter, D., 2000. Redefining the genus *Aplanochytrium* (phylum Labyrinthulomycota). *Mycotaxon* 76, 439–444.
- Leander, C., Porter, D., 2001. The Labyrinthulomycota is comprised of three distinct lineages. *Mycologia* 93, 459–464.
- Moro, I., Negrisolo, E., Callegaro, A., Andreoli, C., 2003. *Aplanochytrium stocchinoi*: a new Labyrinthulomycota from the Southern Ocean (Ross Sea, Antarctica). *Protist* 154, 331–340.
- Perkins, F.O., 1973. A new species of marine labyrinthulid *Labyrinthuloides yorkensis* gen nov. spec. nov. cytology and fine structure. *Arch. Mikrobiol.* 90, 1–17.
- Perkins, F.O., 1974. Reassignment of *Labyrinthula minuta* to the genus *Labyrinthuloides*. *Mycologia* 66, 697–702.
- Porter, D., 1989. Phylum *Labyrinthulomycota*. In: Margulis, L., Corliss, J.O., Melkonian, M., Chapman, D.J. (Eds.), *Handbook of Protoctista*. Jones and Bartlett, Boston, pp. 388–398.
- Posada, D., Crandall, K.A., 1998. MODELTEST: testing the model of DNA substitution. *Bioinformatics* 14, 817–818.
- Quick, J.A., 1974a. A new marine *Labyrinthula* with unusual locomotion. *Trans. Am. Microsc. Soc.* 93, 52–61.
- Quick, J.A., 1974b. *Labyrinthuloides schizochytrops* n. sp., a new marine labyrinthula with spheroid “spindle” cells. *Trans. Am. Microsc. Soc.* 93, 344–365.
- Raghukumar, S., 2002. Ecology of the marine protists, the Labyrinthulomycetes (Thraustochytrids and Labyrinthulids). *Eur. J. Protistol.* 38, 127–145.
- Strimmer, K., Von Haeseler, A., 1996. Quartet puzzling: a quartet maximum likelihood method for reconstructing tree topologies. *Mol. Biol. Evol.* 13, 964–969.
- Swofford, D.L., 1999. *Phylogenetic analysis using parsimony (and other methods) PAUP\* 4.0*. Sinauer Associates, Inc., Sunderland, MA.
- Ulken, A., Jäckle, I., Bahnweg, G., 1985. Morphology, nutrition and taxonomy of an *Aplanochytrium* sp. from the Sargasso Sea. *Mar. Biol.* 85, 89–95.
- Watson, S.W., Raper, K.B., 1957. *Labyrinthula minuta* n. sp. *J. Gen. Microbiol.* 17, 368–377.
- Wethered, J.M., Jennings, D.H., 1985. Major solutes contributing to solute potential of *Thraustochytrium aureum* and *T. roseum* after growth in media of different salinities. *Trans. Br. Mycol. Soc.* 85, 439–446.
- White, T.J., Bruns, T., Lee, S., Taylor, J., 1990. Amplification and direct sequencing of fungal ribosomal RNA genes for phylogenetics. In: Innis, M.A., Gelfand, D.H., Sninsky, J.J., White, T.J. (Eds.), *PCR Protocols: A Guide to Methods and Applications*. Academic Press, San Diego, pp. 315–322.